Oil Palm Shell Nanofiller in Seaweed-based Composite Film: Mechanical, Physical, and Morphological Properties

Abdul Khalil, H.P.S.,[a,*] Ying Ying Tye,[a] Zhari Ismail,[b] Jye Yin Leong,[a] Chaturbhuj K. Saurabh,[a] Tze Kiat Lai,[a] Eunice Wan Ni Chong,[a] P. Aditiawati,[c] Paridah Md. Tahir,[d] and Rudi Dungani [c]

Composite films that utilize seaweed as a matrix and oil palm shell (OPS) nanoparticles as a reinforcing material were developed. The effects of loading OPS nanoparticle (0%, 1%, 5%, 10%, 20%, and 30%) into seaweed films were determined by analyzing the physical, mechanical, and morphological properties of the films. The seaweed-based film incorporated with OPS nanoparticles at a high concentration (20% w/w) achieved the highest tensile strength (44.8 MPa) and Young's Modulus (3.13 GPa). However, the film's hydrophobicity (contact angle = 47.3º) and percentage of elongation at break (2.10%) were reduced. Moreover, it was observed that excessive loading of nanofillers (> 20%) reduced the tensile strength and hydrophilicity of the film. This phenomenon was attributed to the agglomeration of OPS nanoparticles and the formation of large voids on the film surface. Thus, the relative effectiveness of the various tested nanofiller contents in enhancing the mechanical strength of the composite film were found to be ranked in the following order: 20%, 10%, 5%, 30%, and 1%.

Keywords: Seaweed film; Oil palm shell nanoparticles; Nanocomposite; Mechanical; SEM; Contact Angle

*Contact information: a: School of Industrial Technology, Universiti Sains Malaysia, 11800 Penang, Malaysia; b: Department of Pharmaceutical Chemistry, School of Pharmaceutical Sciences, Universiti Sains Malaysia, Minden, Penang 11800, Malaysia; c: School of Life Sciences and Technology, Institut Teknologi Bandung, Gedung Labtex XI, Jalan Ganesha 10, Bandung 40132, West Java, Indonesia; and d: Institute of Tropical Forestry and Forest Products (INTROP), Universiti Putra Malaysia, 43400 Serdang, Selangor, Malaysia; *Corresponding author: akhalilhps@gmail.com*

INTRODUCTION

Various studies have focused on biopolymers due to their biodegradability and derivability from renewable resources (Kuorwel *et al.* 2011). Among the renewable and biodegradable polymers, polysaccharide-based polymers are widely reported to have good mechanical and water barrier properties (Huq *et al.* 2012). Seaweed, one type of polysaccharide biomass, has been recommended by various researchers for the production of biodegradable films due to its unique colloidal properties (Rojas-Graü *et al.* 2007; Siah *et al.* 2015). The most frequently studied seaweed films are prepared from the seaweed-derived polymers such as alginate, carrageenan, and agar. Films developed from such biopolymers exhibit excellent transparency, mechanical strength, and water vapor barrier properties (Rojas-Graü *et al.* 2007; Rhim 2012; Paula *et al*. 2015; Siah *et al.* 2015). However, the production of seaweed-derived polymers is neither economically feasible nor environmentally friendly due to high chemical and energy consumption during the seaweed hydrocolloid extraction process. Therefore, polymer film produced directly from the original form of seaweed is recommended, as the material preparation

of raw seaweed is more simple, environmentally friendly, and cheaper than the seaweed-derived polymers (Siah *et al*. 2015; Abdul Khalil *et al.* 2017). Abdul Khalil and co-workers (2016) also reported that composite films prepared from pure seaweed reinforced with cellulose pulp fibers possessed excellent mechanical strength with acceptable hydrophilicity such that the obtained films could potentially be used for packaging applications.

The oil palm is the world's leading source of vegetable oil and fat, and this resource is capable of producing more than 50 million tons of palm oil annually. A tremendous amount of biomass waste is generated from the oil palm industry, including mesocarp fibers, shells, empty fruit bunches, fronds, and trunks. Oil palm shell (OPS) accounts for approximately 6% of the total amount of generated oil palm waste (Tye *et al*. 2016). The OPS plays an important role as fuel for heat generation, as thermal insulation, for carbon activation for water purification, as a concrete in the building industry, and in automobile disk brake pads (Dagwa *et al*. 2012). Recently, the potential of OPS as a novel filler in composites was studied (Dungani *et al.* 2013; Mohaiyiddin *et al.* 2013; Rosamah *et al*. 2016; Sahari and Maleque 2016). The addition of OPS to polypropylene matrices improved the mechanical properties of the composites, including the tensile strength, elongation at break, and impact strength (Mohaiyiddin *et al.* 2013).

Over the past few years, nanoparticles have been broadly regarded as a potential filler that could improve the physical and mechanical properties of polymer composites (Njuguna *et al.* 2008). Nevertheless, there is still no report regarding the utilization of OPS as a nanofiller in composites based on biopolymer matrixes. Hence, in this study, a new nanocomposite film based on seaweed and OPS nanoparticles was developed. The effects of OPS nanoparticles in seaweed-based film were determined based on mechanical, physical, and morphological tests.

EXPERIMENTAL

Materials

Oil palm shell (OPS) chips were collected from the Ulu Keratong palm oil mill in Johor, Malaysia. Dry seaweed was obtained from Semporna in Sabah, Malaysia. The obtained seaweed was soaked in boiled distilled water and then washed thoroughly with distilled water to remove debris and salt prior to use.

Methods

Preparation of OPS nanofillers

The OPS chips collected from the oil palm processing mill were first ground into granular particles in a Wiley mill. After milling, the granular OPS was sieved (60-mesh size) to separate micro-sized particles such as sand, stone, and micro particles. The sieved OPS was then oven-dried at 110 °C for 24 h to reduce its moisture content. The dried OPS was ground and further sieved to obtain a particle size fraction of 2 µm to 2.8 µm. Using a 0.25-mm MF-sieve, the 20 µm OPS was ground four additional times (Abdul Khalil *et al.* 2011; Rosamah *et al.* 2016).

The fine OPS powder was further ground in a refiner/grinder by means of high-energy ball milling for 30 h at 170 rpm. The ball mill was characterized by a ball-to-powder weight ratio of 10:1, a stainless steel chamber, and stainless steel balls with diameters of 19 mm, 12.7 mm, and 9.5 mm. The samples were oven-dried and kept at

110 °C in the oven for 24 h to prevent agglomeration and contact with moisture (Abdul Khalil *et al.* 2011; Rosamah *et al.* 2016).

Characterization of OPS nanoparticles

The distribution of OPS nanoparticles was studied using particle size analyzer (Zetasizer Ver. 6.11, Malvern, UK) by means of dynamic light scattering measurements using a 532-nm laser. The analysis was repeated three times using the equipment's internal setting. In addition, the particle size of OPS particles was measured using a transmission electron microscope (TEM). The dried OPS nanoparticles were first dissolved in acetone and dispersed with an ultrasonicator for 10 min. Next, a drop of the dissolved nanoparticle solution was placed on the dull surface of the copper grids. The copper grids containing the sample were then viewed under energy-filtering TEM (Zeiss Libra® 120, Oberkochen, Germany) at certain magnifications.

Preparation of seaweed/OPS nanocomposite films

The seaweed/OPS nanocomposite films were prepared by casting method. A 2% (w/v) aqueous seaweed solution was prepared by soaking in distilled water overnight and mixed with different concentrations (0%, 1%, 5%, 10%, 20%, and 30% w/w) of OPS nanoparticles (calculated based on wt.% of seaweed). The obtained mixture was heated below 100 ºC to prevent the thermal degradation of the nanofillers while being occasionally stirred to prevent the hardening of the solution (Abdul Khalil *et al*. 2016). After the mixture was completely dissolved, it was poured evenly into a container with dimensions of 21 cm × 30 cm × 5 cm and subsequently left to dry at room temperature for 48 h before further characterization.

Methods

Characterization of seaweed/OPS nanocomposite films-physical properties

The thicknesses of the nanocomposite films were determined based on TAPPI T411 om-89 (1997). A precision micrometer (Mitutoyo, Kanagawa, Japan) was used to measure the film's thicknesses. The value was set to zero before the readings were recorded. Six thickness measurements were taken at various positions on each specimen, and the average values were recorded. The readings were recorded in micrometers (µm) and presented as the mean ± standard deviation.

To examine the surface wettability of the films, the static water contact angles of the films were measured at room temperature by the drop method using a KSV CAM 101 (KSV Instruments Ltd., Finland) optical contact angle meter. A drop of water was formed on the surface with a hypodermic syringe, which was operated through micrometer screw control to slowly withdraw the tip of the syringe from the drop while the water was being ejected and the drop was growing. The image was recorded for 25 s at a speed of one frame every 5 s. The contact angles were measured on both sides of the drop and averaged. Each reported contact angle was the mean value of at least 10 measurements.

Mechanical properties

The procedure used to prepare the nanocomposite films to test their mechanical properties was adapted from ASTM D882-02 (2002). Tensile tests were run using a texture analyzer TA.XT plus (Stable Micro System Ltd., Godalming, UK), series No. 11633, with a load cell of 30 kg and a crosshead speed of 10 mm/min. The film samples were cut into rectangles (100 mm × 20 mm) and then clamped between grips, leaving an

initial distance between the grips of 60 mm. The tensile strength (MPa) values were calculated by dividing the maximum load (N) necessary to pull the sample film apart by the cross-sectional area (mm^2). The percentage of elongation at break was calculated by dividing the film elongation at the moment of rupture by the initial grip length of the samples, multiplied by 100.

Meanwhile, the Young's modulus (GPa) was calculated by drawing a tangent to the initial linear portion of the stress-strain curve, selecting any point of this tangent, and dividing the tensile stress by the corresponding strain. A total of 6 samples were tested for each film type, and the results are presented as the mean ± standard deviation.

Morphological properties

The surface morphology and tensile fracture surface morphology of the nanocomposite films were examined using a scanning electron microscope (SEM), model EVO MA10, Carl-ZEISS SMT, Oberkochen, Germany. The samples were placed onto an SEM holder that used double-sided electrically conducting carbon adhesive tapes to avoid surface charges on the specimens when exposing them to the electron beam. The specimens were then coated with a thin gold-palladium layer using a Polaron SC515 sputter coater (Fisons Instruments, Loughborough, UK). The SEM applied a focused beam of high-energy electrons to produce a variety of signals at the surfaces of the solid specimens.

Statistical analysis

DSAASTAT ver. 1.101 by Andrea Onofri (Perugia, Italy) was used for the statistical analysis of all data from each testing. The data were analyzed by an analysis of variance (ANOVA), and multiple comparisons of means were conducted using Tukey's test.

RESULTS AND DISCUSSION

Characterization of OPS Nanoparticles

The OPS particles were converted into nanoparticles by means of ball milling. Figure 1a presents the wide particle size distribution range of the OPS nanoparticles, which was determined using the particle size analyzer.

According to Fig. 1a, the nanosize distribution intensity of the OPS particles reached approximately 90%, in which the average diameters of the OPS particles were between 1 nm and 100 nm. Therefore, this result indicated that most of the OPS particle sizes had been reduced to the nanoscale based on the high nanosize distribution intensity shown.

In addition, the sizes and shapes of the OPS particles were examined by TEM. A typical TEM image of OPS is shown in Fig. 1b. From the TEM images, it was apparent that the OPS particles were spherical and nano-scaled (as indicated by the arrows in Fig. 1b). Hence, both analyses indicated that the OPS particles were within the nano size domain. These observations were also verified by Rosamah *et al.* (2016), who showed that OPS nanoparticles could be produced from raw OPS by using a high-energy ball milling process.

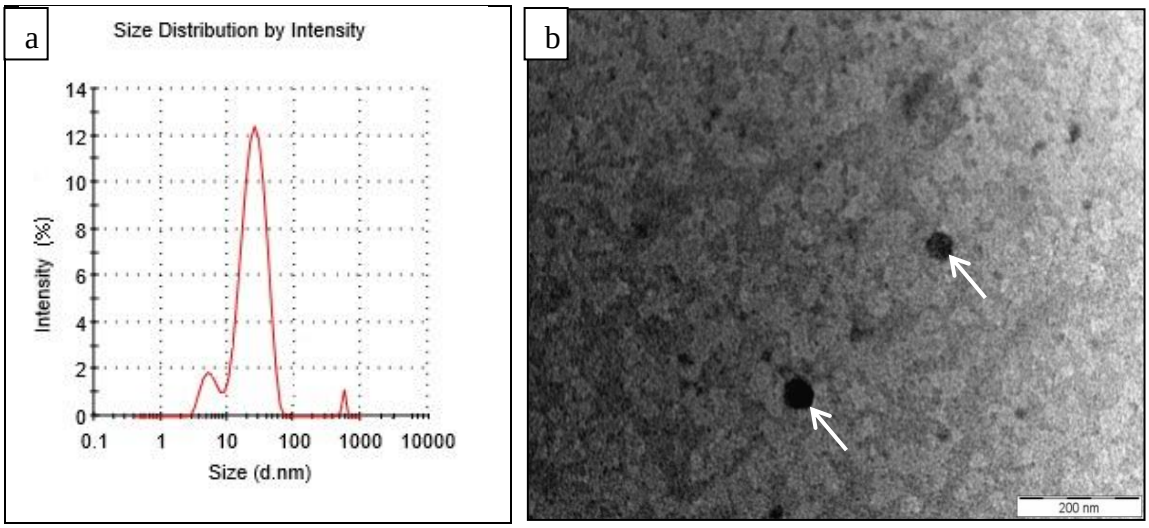

Fig. 1. Particle size analysis of OPS nanoparticles: (a) Particle size distribution of OPS nanoparticles and (b) TEM micrograph of OPS nanoparticles

Effects of OPS Nanoparticle Reinforcement on Seaweed-based Biodegradable Films

Thickness and opacity of bio-nanocomposite films

Table 1 shows the thicknesses of the seaweed and seaweed/OPS nanoparticle composite films. The thickness of the neat seaweed film was 79.1 µm ± 0.47 µm. According to Table 1, the thickness of the films slightly increased with increased OPS nanofiller content, due to the increased solids content (Shankar and Rhim 2016).

Moreover, the opacity of the films also increased as the concentration of OPS nanofillers increased (Fig. 2). Atef *et al.* (2015) reported that the thickness of a film could affect the transparency of the film. Therefore, the incorporation of a greater number of nanofillers into the seaweed matrix corresponded with darker films, as shown in Fig. 2.

Table 1. Thickness, Tensile Strength, Young Modulus, and Elongation at Break of Seaweed Films Incorporated with or without OPS Nanofillers

Film	Thickness (µm)	Tensile Strength (MPa)	Young Modulus (GPa)	Elongation at Break (%)
Blank	79.1 ± 0.47^{a}	31.4 ± 0.32^{a}	2.15 ± 0.01^{a}	3.30 ± 0.35^{a}
1%	82.3 ± 0.32^{b}	33.0 ± 0.49^{b}	2.15 ± 0.01^{a}	2.72 ± 0.45^{a}
5%	83.2 ± 0.19^{b,c}	39.2 ± 0.44^{d}	2.28 ± 0.01^{a}	2.45 ± 0.40^{a,b}
10%	83.8 ± 0.11^{c}	40.4 ± 0.52^{e}	3.00 ± 0.14^{b}	2.20 ± 0.49^{a,b}
20%	84.1 ± 0.12^{c}	44.8 ± 0.39^{f}	3.13 ± 0.01^{b}	2.10 ± 0.33^{a,b}
30%	89.0 ± 1.13^{d}	34.3 ± 0.48^{c}	2.98 ± 0.25^{b}	2.08 ± 0.46^{b}

$^{a, b, c, d, e, f}$ Values along each row with the same letter are not significantly ($p > 0.05$) different as analyzed by Tukey's Test

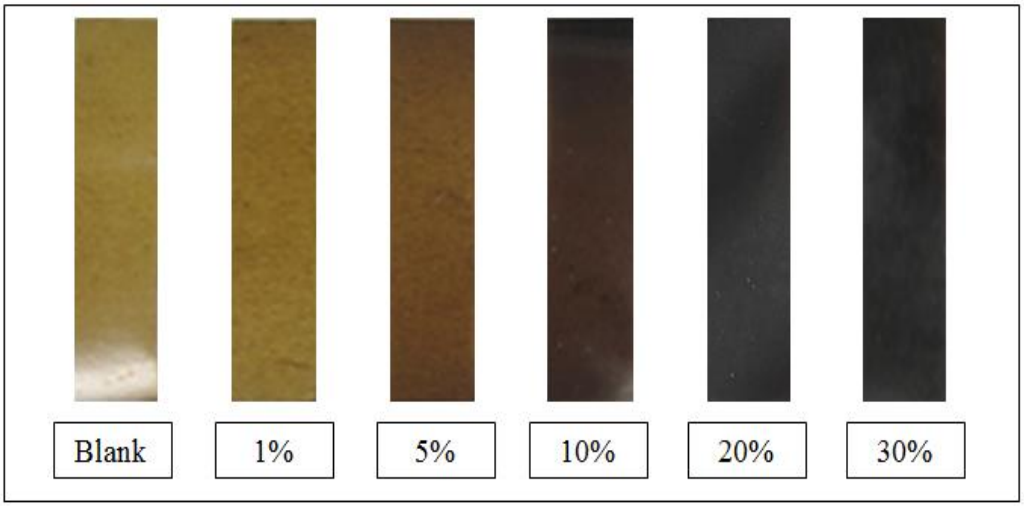

Fig. 2. Seaweed films incorporated with or without OPS nanofillers

Hydrophilicity of bio-nanocomposite films

A contact angle analysis is used to determine the wettability of a liquid on a solid surface. The contact angle, θ, is the angle formed by a liquid drop at the intersection point of the three-phase boundary between the planes tangent to the liquid and solid surfaces. When a liquid drop remains on a solid surface, its three balancing forces (the interfacial tensions between the solid and liquid (SL), the interfacial tensions between the solid and vapor (SV), and the interfacial tensions between the liquid and vapor (LV)) are in equilibrium. High values of θ indicate weak interaction and poor wetting (Ucar *et al.* 2010). In terms of energetics, this result indicates that the cohesive forces associated with bulk water are greater than the forces associated with the interaction of water with the surface (Arkles 2011). In contrast, low values of θ indicate a strong liquid-solid interaction, such that the liquid tends to wet or spread out on the solid (Ucar *et al.* 2010). This result indicates that the forces associated with the interaction of water with the surface are greater than the cohesive forces associated with bulk liquid water (Arkles 2011). The solid surface should be rigid, smooth, and homogeneous for the determination of the contact angle with that particular solid (Tavana *et al.* 2005).

The contact angle of the blank seaweed film was 62.3° (Fig. 3a). Generally, films with water contact angles greater than 65° are considered to be hydrophobic (Shankar and Rhim 2016). Therefore, the raw seaweed film was hydrophilic in this study. This phenomenon was due to seaweed polysaccharide exhibited large number of hydroxyl groups, which could increases the polar component of the surface free energy and then results in an increase in the hydrophilicity of the films (Saha and Bhattacharya 2010; Rhim *et al.* 2011; Tabei *et al.* 2011; Kadam *et al.* 2015). According to Fig. 3, the contact angle of the nanocomposite films decreased when the nanofiller content increased. The nanocomposite film with 20% of nanofillers incorporated obtained the lowest contact angle (47.2°). The OPS nanofillers were basically hydrophilic. According to Husseinsyah *et al.* (2014), OPS consists of many hydroxyl groups that contribute to its hydrophilic nature because it has a high tendency to absorb water. Therefore, the addition of OPS nanofillers increased the number of hydroxyl groups in the matrix and caused the nanocomposite films to become more accessible to water. Hence, the increase in nanofiller content decreased the contact angle of the nanocomposite film and increased the hydrophilicity of the film surface.

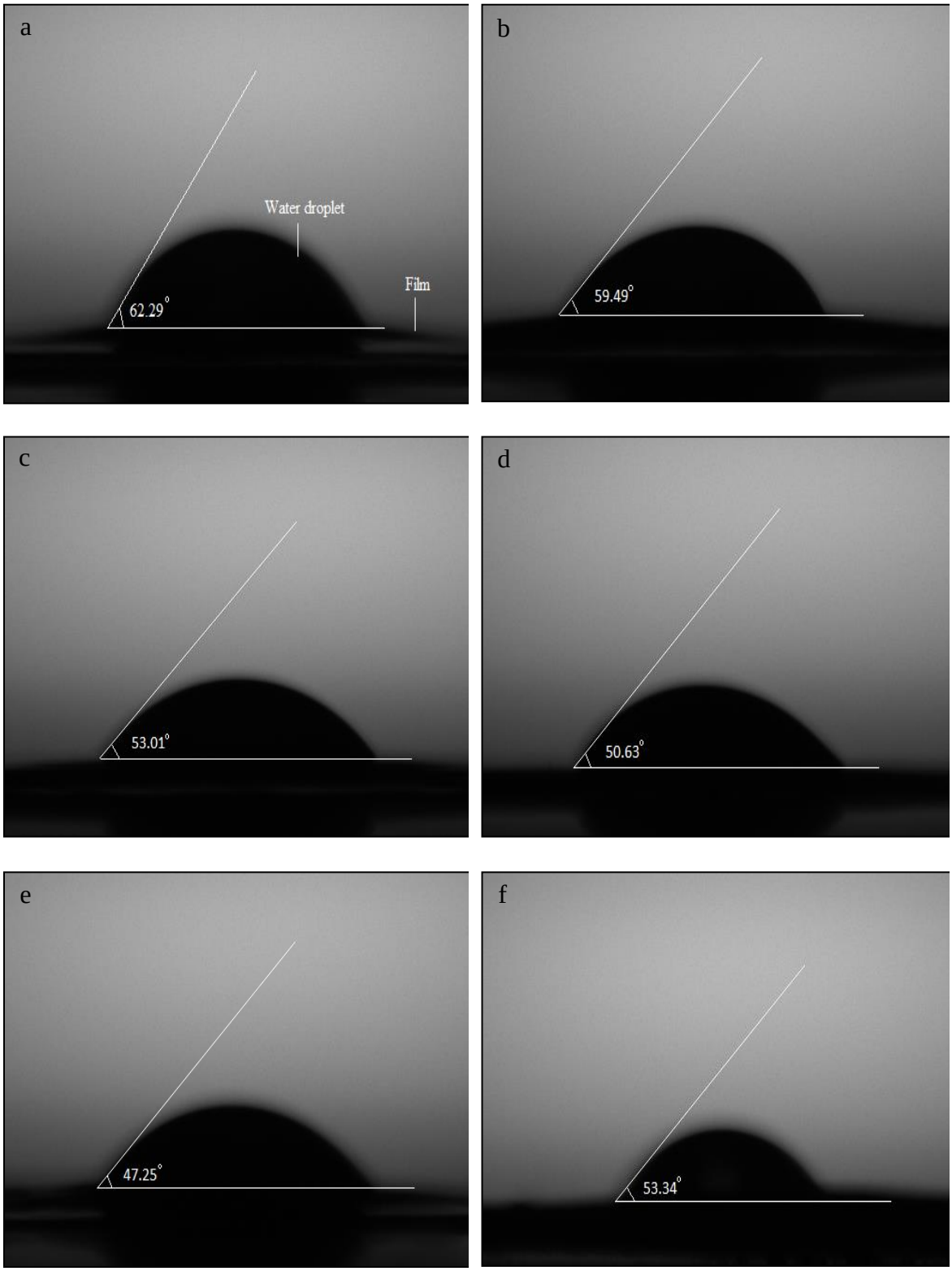

Fig. 3. Contact angle of seaweed films with varying degrees of incorporation of OPS nanofillers: (a) blank, (b) 1%, (c) 5%, (d) 10%, (e) 20%, and (f) 30%

In contrast, the contact angles of the nanocomposite films increased when more than 20% of nanoparticles were added to the seaweed matrix (Fig. 3f). It has been observed that excessive amount of OPS nanoparticle incorporated could cause agglomeration of the nanofillers, and this could account for the poor wetting of the polymer systems (Rosamah *et al.* 2016). Thus, this phenomenon could be further verified by SEM.

Mechanical properties of bio-nanocomposite films

Tensile strength (TS) is the maximum tensile stress withstood by a sample during the tension test. If the maximum tensile stress occurs at either the yield point or the break point, it is designated as the tensile strength at yield or at breaking, respectively. The TS of the seaweed film (blank) was the lowest at 31.4 MPa. In addition, the TS of the nanocomposite film increased with increased OPS nanofiller content (Table 1). The maximum TS was observed at 20% of the OPS nanofiller, which was at approximately 44.8 MPa. This finding indicated that good compatibility between the seaweed and the OPS nanofillers was achieved, in which the TS of the nanocomposite films were enhanced by the presence of OPS nanoparticles compared to the blank seaweed film. This phenomenon could be due to the high specific surface area and uniform dispersion of the nanoparticles in the matrix, and good bonding between the hydrophilic oil palm nanoparticles and seaweed with the presence of hydroxyl groups (-OH groups), which could provide better filler-matrix interfacial interactions and also allow for the effective transfer of stress through a shear mechanism from the matrix to the particles (Huq *et al.* 2012; Khan *et al.* 2012; Mohaiyiddin *et al.* 2013; Zarina and Ahmad 2014; Rosamah *et al.* 2016; Abdul Khalil *et al.* 2016). Hence, it was believed that the nanocomposite film could sustain greater loads when up to 20% of OPS nanofillers were incorporated. A similar finding was reported by Piyada *et al.* (2013), wherein the highest TS was obtained when 20% of starch nanocrystals were loaded in a composite film.

Surprisingly, when the OPS nanofiller content exceeded 20% in the composite film, the TS of the nanocomposite film tended to decrease to a level even lower than that of the blank seaweed film (Table 1). TS was reduced basically due to the agglomeration of nanofillers in the seaweed matrix, which caused filler-filler interaction instead of filler-matrix interaction (Johar and Ahmad 2012). Therefore, it was believed that the poor filler-matrix interfacial interaction was formed in this case. Rosamah and co-workers (2016) reported that poor filler-matrix interfacial interaction could affect the stress transfer mechanism and cause poor wetting of the biopolymer system. The poor wetting between the nanoparticles and matrix could result in a higher tendency to form voids in the composite film; such voids act as stress points, and consequently, this phenomenon lead to the reduction in the tensile properties of the composite films.

Young's Modulus (YM) measures the resistance of a material to elastic deformation under load, which means a stiff material has a high YM whereas a flexible material has a low YM. Based on Table 1, the YM value of the blank seaweed film was 2.15 GPa, which was higher than those seaweed-derived polymers such as alginate (1.88 GPa), carrageenan (1.1 GPa), and agar (1.3 GPa) (Ghosh *et al.* 2010; Shankar *et al.* 2015, 2016). However, the addition of OPS nanofillers up to 5% did not lead to significantly different YM values in the composite film as compared to the control film. The YM of the seaweed film increased when more than 10% of the OPS nanoparticles were incorporated. This phenomenon indicated that the reinforcing effect of OPS nanofillers at

a concentration of 10% or higher was sufficient to improve the mechanical properties of the biopolymer (seaweed) composite film.

Elongation at break indicates a film's stretchability (extensibility) and flexibility, and is determined when the film breaks under tensile testing and is expressed as the percentage of extension or stretch from the original length of the film. According to the results presented in Table 1, the increase in OPS nanofiller content decreased the elongation at break of all nanocomposite films. In contrast, the blank seaweed film demonstrated the highest percentage of elongation at break, approximately 3.30%. This finding indicated that the incorporation of OPS nanofillers reduced the flexibility (or increased the brittleness) of the composite films. Because the OPS nanofillers were more rigid than the seaweed matrix, the increase in nanofiller content would restrict the chain mobility of the matrix available for elongation and cause a decrease in the deformability of the interface between the filler and the matrix (Rosamah *et al.* 2016). Hence, this phenomenon was attributed to a higher breaking tendency (lower deformation) of the nanocomposite films in comparison to the blank seaweed film. Additionally, it was found that the composite film with 30% nano-OPS loading had the lowest elongation at break value; it was the only sample that was significantly different ($p < 0.05$) from the blank seaweed film.

Surface morphology of bio-nanocomposite films

To observe the dispersion level of OPS nanofillers, the homogeneity of the composite, and the presence of agglomeration of OPS nanofillers in the matrix, SEM was used to analyse the morphological surface of the composite films. The morphologies of the nanocomposite films that incorporated different OPS nanofiller contents are shown in Figs. 4(a though f). The surface of the blank seaweed film was relatively smooth. In contrast, the surfaces of the nanocomposite films became rougher with increased OPS nanofiller content. Nevertheless, additions of up to 20% OPS nanofillers were well dispersed and distributed in the seaweed matrix. No obvious aggregations of OPS nanofillers or microphase separation were observed (Figs. 4b through e). Hence, good mechanical strength (*i.e.*, tensile strength) was attained (Table 1).

Interestingly, nanocomposite films with 30% OPS nanofiller content exhibited poor dispersion of the OPS nanofillers in the seaweed-based biocomposite films due to the agglomeration of nanofillers. Sanchez-Garcia *et al.* (2010) reported that the agglomeration of nanofillers was attributed to the self-association of the nanofillers *via* hydrogen bonding. Nanofiller agglomeration could reduce the interfacial contact between the nanofillers and the matrix and thus result in poor interfacial stress transfer. Therefore, this finding showed that seaweed was not compatible with nanofillers in this ratio, the film of which possessed poor mechanical strength, as shown in Table 1. Because low nanoparticle contents dispersed more homogenously than high nanoparticle contents in the seaweed matrix (Figs. 4b through f), the nanoparticles are able to form stronger interactions and adhesions on the interfaces of the filler and matrix (Chen *et al.* 2008; Piyada *et al.* 2013). Hence, the mechanical strength of the composite films was enhanced (Table 1).

Fracture surface morphology of bio-nanocomposite films

The tensile strength behavior of the nanocomposite films was further studied by examining the fracture surfaces of these films under SEM. The morphology of the fracture surfaces of various biopolymer films is shown in Fig. 5. The blank seaweed film

showed a fairly smooth fracture surface, which was a common brittle fracture. This indicated that the resistance to crack propagation was lower, which resulted in lower strength. This observation verified that the tensile strength of the blank seaweed film was lower than those films with added OPS nanofillers, as shown in Table 1.

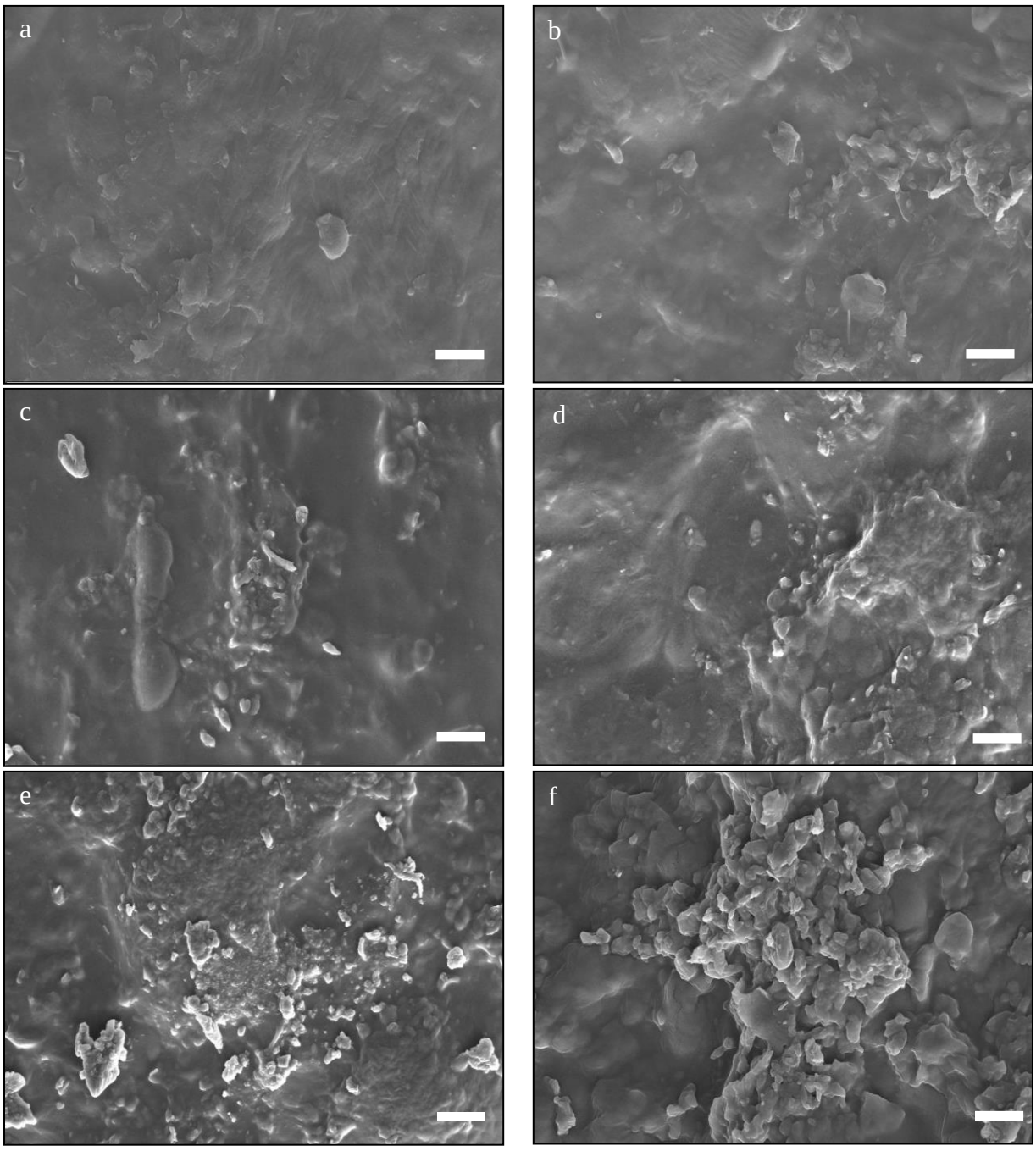

Fig. 4. Scanning electron microscopy images of seaweed films with varying OPS nanofiller content at 1Kx (scale bar, 2 µm): (a) blank, (b) 1%, (c) 5%, (d) 10%, (e) 20%, and (f) 30%

The tensile fracture surface appearance changed after the addition of OPS nanofillers. The fracture surfaces of the nanocomposite films were rough and exhibited ragged waves in which the degree of fracture surface roughness increased in the

following order: blank (without addition of OPS nanofillers), 1%, 5%, 10%, 20%, and 30% (Fig. 5). The rougher the fracture surface was, the higher the crack resistance was. Therefore, more energy or force was required to propagate cracks (Voo *et al*. 2011). However, when the seaweed film incorporated 30% OPS nanofillers, more voids and cavities were formed in these films compared to the other filled nanocomposite films (Fig. 5f). The large void space actually indicated a poorer filler-matrix interaction. Hence, it was suspected that the voids and cavities surrounding the fillers might be one of the reasons that caused the reduction in the tensile strength of the bio-nanocomposite film, as discussed earlier.

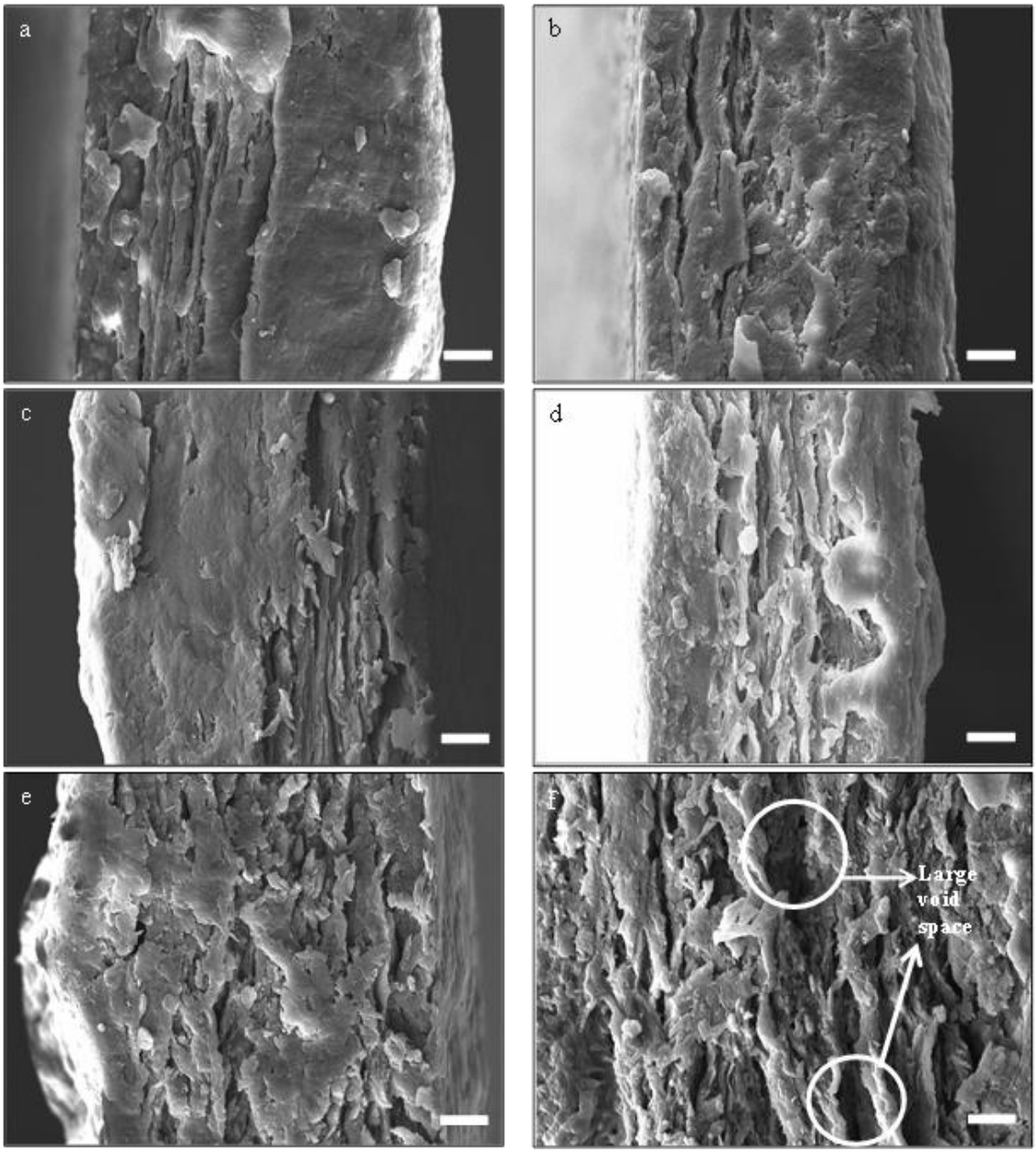

Fig. 5 SEM images of fracture surfaces of tensile test specimens for seaweed films with varying incorporation of OPS nanofillers at 1Kx (scale bar, 2 µm): (a) blank, (b) 1%, (c) 5%, (d) 10%, (e) 20%, and (f) 30%

CONCLUSIONS

1. When reinforced with OPS nanoparticles, the physical, mechanical, and morphological properties of seaweed-based films were changed remarkably.
2. The mechanical properties (except elongation at break) of nano-OPS/seaweed composite films increased with the increase in OPS nanofiller content.
3. The surfaces of the nano-OPS/seaweed composite films became more hydrophilic with the increase in OPS nanofiller content.
4. The SEM analysis revealed no aggregations of fillers and an absence of void formation in the composite film when up to 20% OPS nanoparticles was incorporated.
5. The OPS nanoparticles can be used as potential reinforcing nanofillers to improve the film properties of biopolymer-based film.

ACKNOWLEDGMENTS

The authors gratefully acknowledge the Ministry of Higher Education for the Fundamental Research Grant Scheme – Malaysia's Rising Star Award 2015 (FRGS-203/PTEKIND/6711531).

REFERENCES CITED

Abdul Khalil, H. P. S., Fizree, H. M., Jawaid, M., and Alattas, O. S. (2011). "Preparation and characterization of nano structured materials from oil palm ash: A bio-agricultural waste from oil palm mill," *BioResources* 6(4), 4537-4546.

Abdul Khalil, H. P. S., Tye, Y. Y., Chow, S. T., Saurabh, C. K., Paridah, M. T., Dungani, R., and Syakir, M. I. (2016) "Cellulosic pulp fiber as reinforcement materials in seaweed-based film," *BioResources* 12(1), 29-42.

Abdul Khalil, H. P. S., Tye, Y. Y., Saurabh, C. K., Leh, C.P., Lai, T. K., Chong, E. W., Nurul Fazita, M. N., Hafiidz, J. M., Banerjee, A., Syakir, M. I. (2017) "Biodegradable polymer films from seaweed polysaccharides: A review on cellulose as a reinforcement material," *Express Polymer Letters* 11(4), 244-265.

Arkles, B. (2011). *Hydrophobicity, Hydrophilicity, and Silane Surface Modification*, Gelest Inc., Morrisville, NC, USA.

ASTM D882-02 (2002). "Standard test methods for tensile properties of thin plastics sheeting," ASTM International, West Conshohocken, PA.

Atef, M., Rezaei, M., and Behrooz, R. (2015). "Characterization of physical, mechanical, and antibacterial properties of agar-cellulose bionanocomposite films incorporated with savory essential oil," *Food Hydrocolloids* 45, 150-157. DOI: 10.1016/j.foodhyd.2014.09.037

Chen, Y., Cao, X., Chang, P. R., and Huneault, M. A. (2008). "Comparative study on the films of poly (vinyl alcohol)/pea starch nanocrystals and poly (vinyl alcohol)/native pea starch," *Carbohydrate Polymers* 73(1), 8-17. DOI: 10.1016/j.carbpol.2007.10.015

Dagwa, I. M., Builders, P. F., and Achebo, J. (2012). "Characterization of palm kernel shell powder for use in polymer matrix composites," *International Journal of Mechanical Engineering and Mechatronics* 12(04), 88-93.

Dungani, R., Islam, M. N., Abdul Khalil, H. P. S., Davoudpour, Y., and Rumidatul, A. (2013). "Modification of the inner part of the oil palm trunk (OPT) with oil palm shell (OPS) nanoparticles and phenol formaldehyde (PF) resin: Physical, mechanical, and thermal properties," *BioResources* 9(1), 455-471.

Ghosh, S., Kaushik, R., Nagalakshmi, K., Hoti, S. L., Menezes, G. A., Harish, B. N., and Vasan, H. N. (2010). "Antimicrobial activity of highly stable silver nanoparticles embedded in agar-agar matrix as a thin film," *Carbohydrate Research* 345(15), 2220-2227.

Huq, T., Salmieri, S., Khan, A., Khan, R. A., Le Tien, C., Riedl, B., Fraschini, C., Bouchard, J., Uribe-Calderon, J., Kamal, M. R., and Lacroix, M. (2012). "Nanocrystalline cellulose (NCC) reinforced alginate based biodegradable nanocomposite film," *Carbohydrate Polymers* 90(4), 1757-1763. DOI: 10.1016/j.carbpol.2012.07.065

Husseinsyah, S., Seong Chun, K., Hadi, A., and Ahmad, R. (2014). "Effect of filler loading and coconut oil coupling agent on properties of low-density polyethylene and palm kernel shell eco-composites," *Journal of Vinyl and Additive Technology* 22(3), 200-205. DOI: 10.1002/vnl.21423

Johar, N., and Ahmad, I. (2012). "Morphological, thermal, and mechanical properties of starch biocomposite films reinforced by cellulose nanocrystals from rice husks," *BioResources* 7(4), 5469-5477.

Kadam, S. U., Pankaj, S. K., Tiwari, B. K., Cullen, P. J., and O'Donnell, C. P. (2015). "Development of biopolymer-based gelatin and casein films incorporating brown seaweed *Ascophyllum nodosum* extract," *Food Packaging and Shelf Life* 6, 68-74. DOI: 10.1016/j.fpsl.2015.09.003

Khan, A., Khan, R. A., Salmieri, S., Le Tien, C., Riedl, B., Bouchard, J., Chauve, G., Tan, V., Kamal, M. R., and Lacroix, M. (2012). "Mechanical and barrier properties of nanocrystalline cellulose reinforced chitosan based nanocomposite films," *Carbohydrate Polymers* 90(4), 1601-1608. DOI: 10.1016/j.carbpol.2012.07.037

Kuorwel, K. K., Cran, M. J., Sonneveld, K., Miltz J., and Bigger, S. W. (2011). "Antimicrobial activity of biodegradable polysaccharide and protein-based films containing active agents," *Journal of Food Science* 76(3), R90-R102. DOI: 10.1111/j.1750-3841.2011.02102.x

Mohaiyiddin, M. S., Ong, L. H., and Akil, H. M. (2013). "Preparation and characterization of palm kernel shell/polypropylene biocomposites and their hybrid composites with nanosilica," *BioResources* 8(2), 1539-1550.

Njuguna, J., Pielichowski, K., and Desai, S. (2008). "Nanofiller-reinforced polymer nanocomposites," *Polymers for Advanced Technologies* 19(8), 947-959. DOI: 10.1002/pat.1074

Paula, G. A., Benevides, N. M. B., Cunha, A. P., de Oliveira, A. V., Pinto, A. M. B., Morais, J. P. S., and Azeredo, H. M. C. (2015). "Development and characterization of edible films from mixtures of k-carrageenan, i-carrageenan, and alginate," *Food Hydrocolloids* 47, 140-145. DOI: 10.1016/j.foodhyd.2015.01.004

Piyada, K., Waranyou, S., and Thawien, W. (2013). "Mechanical, thermal and structural properties of rice starch films reinforced with rice starch nanocrystals," *International Food Research Journal* 20(1), 439-449.

Rhim, J. W. (2012). "Physical-mechanical properties of agar/κ-carrageenan blend film and derived clay nanocomposite film," *Journal of Food Science* 77(12), N66-N73. DOI: 10.1111/j.1750-3841.2012.02988.x

Rhim, J. W., Lee, S. B., and Hong, S. I. (2011). "Preparation and characterization of agar/clay nanocomposite films: The effect of clay type," *Journal of Food Science* 76(3), N40-N48. DOI: 10.1111/j.1750-3841.2011.02049.x.

Rojas-Graü, M. A., Avena-Bustillos, R. J., Olsen, C., Friedman, M., Henika, P. R., Martín-Belloso, O., Pan, Z., and McHugh, T. H. (2007). "Effects of plant essential oils and oil compounds on mechanical, barrier and antimicrobial properties of alginate-apple puree edible films," *Journal of Food Engineering* 81(3), 634-641. DOI: 10.1016/j.jfoodeng.2007.01.007

Rosamah, E., Hossain, M. S., Abdul Khalil, H. P. S., Wan Nadirah, W. O., Dungani, R., Nur Amiranajwa, A. S., Suraya, N. L. M., Fizree, H. M., and Mohd Omar, A. K. (2016). "Properties enhancement using oil palm shell nanoparticles of fibers reinforced polyester hybrid composites," *Advanced Composite Materials* 1-14. DOI: 10.1080/09243046.2016.1145875

Saha, D., and Bhattacharya, S. (2010). "Hydrocolloids as thickening and gelling agents in food: A critical review," *Journal of Food Science and Technology* 47(6), 587-597. DOI: 10.1007/s13197-010-0162-6

Sahari, J., and Maleque, M. A. (2016). "Mechanical properties of oil palm shell composites," *International Journal of Polymer Science* 1-7. DOI: 10.1155/2016/7457506

Shankar, S., Reddy, J. P., Rhim, J. W., and Kim, H. Y. (2015). "Preparation, characterization, and antimicrobial activity of chitin nanofibrils reinforced carrageenan nanocomposite films," *Carbohydrate Polymers* 117, 468-475. DOI: 10.1016/j.carbpol.2014.10.010

Shankar, S., and Rhim, J. W. (2016). "Preparation of nanocellulose from micro-crystalline cellulose: The effect on the performance and properties of agar-based composite films," *Carbohydrate Polymers* 135, 18-26. DOI: 10.1016/j.carbpol.2015.08.082

Shankar, S., Wang, L. F., and Rhim, J. W. (2016). "Preparations and characterization of alginate/silver composite films: Effect of types of silver particles," *Carbohydrate Polymers* 146, 208-216. DOI: 10.1016/j.carbpol.2016.03.026

Siah, W. M., Aminah, A., and Ishak, A. (2015). "Edible films from seaweed (*Kappaphycusalvarezii*)," *International Food Research Journal* 22(6), 2230-2236.

TAPPI T411 om-89 (1997). "Thickness (caliper) of paper, paperboard, and combined board," TAPPI Press, Atlanta, GA.

Tabei, Y., Tsutsumi, K., Ogawa, A., Era, M., and Morita, H. (2011). "Application of insoluble fibroin film as conditioning film for biofilm formation," *Sensors and Materials* 23(4), 195-205.

Tavana, H., Petong, N., Hennig, A., Grundke, K., and Neumann, A. W. (2005). "Contact angles and coating film thickness," *The Journal of Adhesion* 81(1), 29-39. DOI: 10.1080/00218460590904435

Tye, Y. Y., Lee, K. T., Wan Abdullah, W. N., and Leh, C. P. (2016). "The world availability of non-wood lignocellulosic biomass for the production of cellulosic ethanol and potential pretreatments for the enhancement of enzymatic saccharification," *Renewable and Sustainable Energy Reviews* 60, 155-172. DOI: 10.1016/j.rser.2016.01.072

Ucar, I. O., Cansoy, C. E., Erbil, H. Y., Pettitt, M. E., Callow, M. E., and Callow, J. A. (2010). "Effect of contact angle hysteresis on the removal of the sporelings of the green alga Ulva from the fouling-release coatings synthesized from polyolefin polymers," *Biointerphases* 5(3), 75-84. DOI: 10.1116/1.3483467

Voo, R., Mariatti, M., and Sim, L. C. (2011). "Properties of epoxy nanocomposite thin films prepared by spin coating technique," *Journal of Plastic Film & Sheeting* 27(4), 331-346.

Zarina, S., and Ahmad, I. (2014). "Biodegradable composite films based on κ-carrageenan reinforced by cellulose nanocrystal from kenaf fibers," *BioResources* 10(1), 256-271.

Article submitted: March 1, 2017; Peer review completed: June 1, 2017; Revised version received: June 22, 2017; Accepted: June 23, 2017; Published: July 5, 2017.
DOI: 10.15376/biores.12.3.5996-6010